THE JOURNAL OF BIOLOGICAL CHEMISTRY VOL. 282, NO. 36, pp. 26210–26216, September 7, 2007

Establishing an Ion Pair Interaction in the Homomeric ρ1 γ-Aminobutyric Acid Type A Receptor That Contributes to the Gating Pathway*[S]

Received for publication, March 16, 2007, and in revised form, May 30, 2007 Published, JBC Papers in Press, July 2, 2007, DOI 10.1074/jbc.M702314200

Jinti Wang, Henry A. Lester, and Dennis A. Dougherty[1]

From the Division of Chemistry and Chemical Engineering and Division of Biology, California Institute of Technology, Pasadena, California 91125

γ-Aminobutyric acid type A ($GABA_A$) receptors are members of the Cys-loop superfamily of ligand-gated ion channels. Upon agonist binding, the receptor undergoes a structural transition from the closed to the open state, but the mechanism of gating is not well understood. Here we utilized a combination of conventional mutagenesis and the high precision methodology of unnatural amino acid incorporation to study the gating interface of the human homopentameric ρ1 $GABA_A$ receptor. We have identified an ion pair interaction between two conserved charged residues, Glu^{92} in loop 2 of the extracellular domain and Arg^{258} in the pre-M1 region. We hypothesize that the salt bridge exists in the closed state by kinetic measurements and free energy analysis. Several other charged residues at the gating interface are not critical to receptor function, supporting previous conclusions that it is the global charge pattern of the gating interface that controls receptor function in the Cys-loop superfamily.

Fast inhibitory neurotransmission in the adult mammalian central nervous system is primarily mediated by the amino acid γ-aminobutyric acid (GABA).[2] So far, three types of GABA receptors have been identified, termed $GABA_A$, $GABA_B$, and the homopentameric ρ1 $GABA_A$ receptor, also known as $GABA_C$ (1, 2). Although $GABA_B$ is a G protein-coupled receptor, $GABA_A$ and $GABA_C$ receptors are homologous but distinct members of the Cys-loop superfamily of ligand-gated ion channels, which also includes the nicotinic acetylcholine (nAChR), serotonin, and glycine receptors. Members of this superfamily are composed of five subunits arranged around a central ion-conducting pore, with each subunit consisting of a large extracellular domain, four transmembrane helices (M1–M4), and a large intracellular loop. The newest member of this family, the $GABA_C$ receptor (3), is expressed predominantly on retinal neurons, although recent studies indicate a wide distribution throughout the central nervous system (4–6).

The binding of agonist to a Cys-loop receptor triggers a complex structural transition that results in the opening of a "gate," allowing ions to flow through the channel (7). Identifying the linkage pathway has been limited by the lack of a complete atomic-resolution structure of any fast synaptic receptor. However, two breakthroughs have propelled the field into the structural age. The first is determination of the crystal structure of acetylcholine-binding protein (8), which is homologous to the extracellular domain of the nAChR and, by extension, all Cys-loop receptors. This structural template provides critical insights into the nature of the binding site, but, of course, the ion channel and its gate are missing from such structures. Second, a refined electron microscopy structure of the *Torpedo* acetylcholine receptor by Unwin and co-workers (Protein Data Bank code 2BG9) has shed light onto the global structure and has suggested molecular determinants of functional mechanisms in Cys-loop receptors (9–11).

The available structural information reinforced previous conclusions on the modular nature of Cys-loop receptors, with the extracellular domain being well defined and primarily composed of β sheets and the transmembrane domain exclusively α helical. A large number of ionic residues are found where these two domains meet, and many studies have suggested that specific ion pair interactions make important contributions to the gating mechanism (12–16). We have described this region as the "gating interface," and both experiments and analyses across the Cys-loop superfamily showed that, whereas the overall charging pattern of the gating interface is conserved, specific ion pair interactions are not (16, 17). As such, it is risky to conclude that a particular ion pair interaction that may be important in one Cys-loop receptor will be important throughout the superfamily.

An especially prominent ion pair interaction at the gating interface of the *Torpedo* nAChR structure is shown in Fig. 1. The side chains of α subunit residues Glu^{45} in loop 2 and Arg^{209} in the pre-M1 segment are in close proximity, and recent studies by Lee *et al.* (15) establish that they form a salt bridge in muscle-type nAChR. These residues align with Glu^{92} and Arg^{258} in the $GABA_C$ ρ1 subunit (Fig. 1). The $GABA_C$ receptor is distinct in several ways from the muscle-type nAChR. The $GABA_C$ receptor is homopentameric, inhibitory (anion conducting), and displays kinetics on the seconds time scale. The muscle-type nAChR is heteromeric ($(\alpha 1)_2\beta 1\gamma\delta$), excitatory

* This work was supported by National Institutes of Health Grants NS 34407 and NS 11756. The costs of publication of this article were defrayed in part by the payment of page charges. This article must therefore be hereby marked "*advertisement*" in accordance with 18 U.S.C. Section 1734 solely to indicate this fact.

[S] The on-line version of this article (available at http://www.jbc.org) contains supplemental Figs. S1 and S2.

[1] To whom correspondence should be addressed: Division of Chemistry and Chemical Engineering, Caltech, 164-30, Pasadena, CA 91125. Tel.: 626-395-6089; Fax: 626-564-9297; E-mail: dadougherty@caltech.edu.

[2] The abbreviations used are: GABA, γ-aminobutyric acid; ACh, acetylcholine; nAChR, nicotinic acetylcholine receptor; Nha, nitrohomoalanine; TPMPA, (1,2,5,6-tetrahydropyridin-4-yl)methylphosphinic acid.

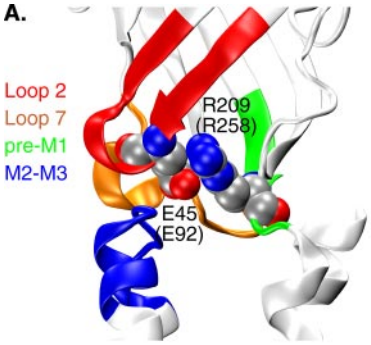

B.

	Loop 2	pre-M1
Tor α	D**E**VNQI	MQ**R**IP
nACh α1	D**E**VNQI	MQ**R**LP
nACh β1	N**E**KDEE	IR**R**KP
nACh γ	N**E**REEA	IQ**R**KP
nACh δ	K**E**VEET	IR**R**KP
nACh α4	D**E**KNQM	IR**R**LP
nACh α7	D**E**KNQV	MR**R**RT
5-HT3A	D**E**KNQV	IR**R**RP
GABA ρ1	S**E**VDMD	LR**R**HI
GABA α1	S**D**HDME	LK**R**KI
GABA α2	S**D**TDME	LK**R**KI
GABA α3	S**D**TDME	LK**R**KI
GABA β1	S**E**VNMD	LK**R**NI
GABA β2	S**E**VNMD	LK**R**NI
Gly α1	A**E**TTMD	LE**R**QM

FIGURE 1. *A*, image showing the proximity of Glu[45] and Arg[209] (space-filling models) in the nAChR. *Numbers* in *parentheses* show the corresponding residues in the GABA$_C$ ρ1 subunit. The structure is the full model of an α subunit of the *Torpedo* nAChR developed by Unwin (9) (PDB code 2BG9). *B*, sequence alignment for loop 2 and pre-M1 (16). All subunits are from human except Tor α (*Torpedo californica*) and nACh α1, β1, γ, and δ, which are mouse muscle. Residues corresponding to Glu[92] and Arg[258] studied here are *bold*.

(cation conducting), and displays kinetics on the milliseconds time scale. Thus we were interested in whether the ion pair interaction seen in the nAChR is also important in the GABA$_C$ receptor. Here we describe studies of this and other potential interactions in the gating interface of the GABA$_C$ receptor using both conventional and unnatural amino acid mutagenesis. We find that GABA$_C$ receptor ρ1 subunits form the same ion pair interaction as previously identified in the nAChR (15). Based on kinetic data, we propose that the salt bridge stabilizes the receptor in the resting state and that agonist binding to the receptor leads to the breaking of the salt bridge, triggering the opening of the ion channel.

MATERIALS AND METHODS

Cloning, Mutagenesis, and mRNA Synthesis—GABA$_C$ receptor subunits were derived from pcDNA3.1 (Invitrogen) containing the complete coding sequence for the human ρ1 receptor subunit, kindly provided by Dr. Sarah C. R. Lummis (University of Cambridge, UK). Wild-type receptor coding sequences were then subcloned into the oocyte expression vector plasmid pGEMHE. The 3′- and 5′-untranslated regions from a *Xenopus* β-globin gene in the vector led to an enhancement of expression by several hundred-fold (18). Mutations in the cDNA were made using the QuikChange mutagenesis kit (Stratagene). Plasmids were linearized with NheI (New England Biolabs, Ipswich, MA) and used as template to produce mRNAs using the T7 mMESSAGE mMACHINE kit from Ambion (Austin, TX). The resulting mRNA is stored at −80 °C.

Electrophysiology and Data Analysis—Stage VI oocytes of *Xenopus laevis* were employed. Electrophysiology recordings were performed 48–72 h after injection in two-electrode voltage clamp mode using the OpusXpress 6000A (Molecular Devices, Axon Instruments, Union City, CA). Holding potentials were −60 mV. Drug applications were 40–130 s in duration. Data were sampled at 125 Hz and filtered at 50 Hz. All drugs were diluted to the desired concentration with ND96 buffer. EC_{50}, IC_{50}, and Hill coefficients were calculated by fitting the does-response relation to the Hill equation (19). All data are reported as mean ± S.E. Maximal currents elicited by GABA, $I_{max(GABA)}$, and by muscimol, $I_{max(muscimol)}$, were measured at saturating concentrations on the same oocytes. The relative efficacy (ϵ), defined as the ratio of $I_{max(muscimol)}/I_{max(GABA)}$, was calculated for each cell then averaged, and is reported as mean ± S.E. All chemicals were purchased from Sigma.

For kinetic measurements, drug applications began at a rate of 0.023 ml/s for 28 s and then decreased to 0.0033 ml/s for 102 s. Measurements of on-kinetics, especially at the higher GABA concentrations, are limited by two factors. The most rapid kinetics was limited by the speed of the drug delivery system. Chamber volume was ~100 μl, so that solution exchange in the entire chamber occurred with a time constant of ~4 s. However, the drug pipette was situated just a few millimeters from the oocyte, so that solution changes were faster near the oocyte; we estimate that the fastest time constant for solution change near the oocyte was 0.5 s. Additional experiments, conducted at exchange rates up to 0.067 ml/s, established that the derived kinetic parameters are not detectably dependent on the rate of drug application. The slowest on-kinetics was limited by the longest drug application time, 130 s (limited by the 1-ml drug reservoir), which allowed for time constants as long as ~44 s. Activation rate constants ($k = 1/\tau$) of ~0.023–2 s^{-1} are therefore in the measurable range. The rate constants k of the individual activation traces were calculated by fitting the activation phase to a first-order exponential function with a sloping baseline (pCLAMP software, Axon Instruments). Values of k were then averaged and plotted against [GABA]; this plot was fitted as a straight line (Fig. 3, *B–E*). The apparent bimolecular binding rate constant k_{act} equals the slope of this plot.

For the deactivation phase, chambers were perfused at 0.05 ml/s until the current returned to the baseline. The rate constants of the individual deactivation traces were calculated by fitting the deactivation phase to a first-order exponential function. The deactivation rate constant was averaged across all GABA concentrations. In general, it was possible to measure kinetics at GABA concentrations in the range of EC_{50} to 10 times EC_{50} (5 times EC_{50} for wild-type receptor). Kinetic parameters are difficult to obtain for lower GABA concentrations because of the small current size.

Unnatural Amino Acid Suppression—Unnatural amino acid, nitrohomoalanine (Nha), was synthesized, conjugated to the dinucleotide deoxycytosine adenosine (dCA), and ligated to truncated 74-nucleotide tRNA as previously described (20). Briefly, the aminoacyl-tRNA was deprotected by photolysis immediately prior to co-injection with mRNA containing an *amber* (TAG) stop codon at position 92. Negative and positive controls were performed as previously reported (21).

Western Blotting—To detect surface expression for several mutants, a hemagglutinin epitope tag was incorporated at the N-terminal in the ρ1 subunit (between positions 2 and 3). Control experiments show a negligible effect of this epitope on EC_{50}. 48–72 h after injection, 12 oocytes were incubated in hypotonic solution (5 mM HEPES, 5 mM NaCl) for 10 min, and then the vitelline/plasma membranes were isolated by physical dissection. The pellet and supernatant were mixed with 5 μl of 2× SDS loading buffer, and SDS-PAGE was performed in 15% Tris-Cl ReadyGels (Bio-Rad Laboratories). The samples were

TABLE 1
Mutations at the gating interface in $GABA_C$ ρ1 subunits

Mutants	EC_{50} for GABA	n_H
	μM	
Wild type	1.34 ± 0.04	2.2 ± 0.1
E92R	N.F.[a]	
E92D	0.03 ± 0.002	1.4 ± 0.1
E92Nha	0.12 ± 0.004	1.6 ± 0.1
D94R	0.3 ± 0.02	2.2 ± 0.2
D96R	5.7 ± 0.5	2.2 ± 0.4
R257D	0.37 ± 0.003	3.5 ± 0.1
R258E	N.E.[b]	
R316D	8.4 ± 0.2	1.6 ± 0.1
K321E	3.3 ± 0.2	2.2 ± 0.2
E92R/R257D	N.S.[c]	
E92R/R258E	0.35 ± 0.004	3.1 ± 0.1
E92R/R316D	N.S.	
E92R/K321E	N.S.	

[a] N.F., nonfunctional; no response to applied GABA, but surface expression of receptor confirmed by Western blot.
[b] N.E., no expression, as confirmed by Western blot.
[c] N.S., no signal; no response to applied GABA, surface expression not independently verified.

subjected to Western blot analysis using the anti-hemagglutinin antibody and visualized using an ECL detection kit (Amersham Biosciences).

RESULTS

Studies of the Human $GABA_C$ Receptor ρ1 Subunit—As in other members of the Cys-loop superfamily, the gating interface of the $GABA_C$ receptor is rich in charged residues. We have studied three positions in loop 2, which frequently has a larger number of charged residues, both by conventional mutagenesis and unnatural amino acid mutagenesis. The results are given in Table 1. In loop 2, Glu^{92} is conserved as negatively charged across the entire Cys-loop family, and it aligns with the previously mentioned αGlu^{45} of the muscle-type nAChR. Its important role in receptor function is confirmed in the $GABA_C$ ρ1 subunit, because the charge reversal mutation E92R gave nonfunctional receptors. Western blot analysis confirms that properly assembled receptors reached the cell surface (supplemental Fig. S1), establishing that the E92R mutation affected receptor function rather than folding, assembly, or trafficking. Previous studies show that introducing a positive charge at this position either lowers the EC_{50} significantly in nAChR and glycine receptor α1 or raises the EC_{50} modestly in $GABA_A$ α1 subunit, demonstrating an important role in gating for this charged residue (12, 14, 16). Two other anionic residues in loop 2 were also probed. Asp-94 is conserved as negatively charged in $GABA_A$ α subunits and nAChR ε, δ, and γ subunits, but not throughout the Cys-loop family; Asp-96 is conserved as negatively charged in all inhibitory Cys-loop receptors. In contrast to E92R, both D94R and D96R are minimally perturbing, consistent with previous observations on the remarkable tolerance in general of the gating interface to such charge reversal mutations (16, 17).

A classic test for a specific ion pair interaction is the charge-swapping experiment; *i.e.* if Glu^{92} experiences an electrostatic interaction with a specific cationic residue, then the nonfunctional E92R mutant often can be "rescued" by converting the cationic partner to an anion. Based on the 2BG9 structure, four positively charged residues could be fairly close to Glu^{92}: Arg^{257} and Arg^{258} in pre-M1 and Arg^{316} and Lys^{321} in the M2–M3 linker. Only Arg^{258} is universally conserved as a positively charged group. The nonfunctional E92R mutant is fully rescued by combination with R258E in pre-M1 but not by R257D, R316D, or K321E. The double mutant E92R/R258E shows a modest 4-fold decrease in EC_{50} (Table 1 and Fig. 2). The single charge reversal mutation R258E produced receptors that cannot traffic to the cell surface, indicating the positive charge is involved in receptor expression, folding, and/or assembly (supplemental Fig. S1). Previous work on the corresponding residue in glycine receptor α1 and nAChR α7 receptors show contributions to agonist potency and efficacy (22, 23). The other three positive sites we studied, Arg^{257}, Arg^{316}, and Lys^{321}, are not critical, because single charge reversal mutations all produced functional receptors with modest shifts in EC_{50}. Therefore, Glu^{92} and Arg^{258} satisfy several criteria expected of residues that lie on the "principal pathway" coupling agonist binding to receptor gating: they are located in close proximity to each other at the gating interface, receptor function can be rescued by charge swapping, and they are conserved in all members of the Cys-loop receptors.

Unnatural Mutant, E92Nha—To explore more fully the role of Glu^{92} in gating, we incorporated an unnatural amino acid that is isosteric and isoelectronic to Glu but does not contain a negative charge. The residue is Nha, the nitro analog of Glu (Fig. 2*C*). Charge neutralization at Glu^{92} would destroy any ion-pairing interaction with Arg^{258}. As shown in Table 1 and Fig. 2*B*, incorporation of Nha at position 92, E92Nha, resulted in an 11-fold *decrease* in EC_{50} for GABA. The E92Nha mutant behavior suggests that charge neutralization greatly affects the salt bridge interaction, producing a gain-of-function channel.

Conventional Mutant, E92D—Because the side-chain length of Asp is one carbon group shorter than that of Glu (Fig. 2*C*), one expects this mutation to weaken the electrostatic interaction with Arg^{258} by moving the two charged groups further apart. Glu^{92} can be replaced by the Asp residue, producing functional receptors with a 40-fold decrease in EC_{50} compared with the wild-type receptors. This apparent gain-of-function mutation also has important mechanistic consequences, as discussed below.

Kinetics of GABA Responses—Fig. 3*A* superimposes normalized waveforms of responses to GABA pulses for wild-type, E92R/R258E, E92Nha, and E92D receptors. Kinetic analysis is simplified by the fact that $GABA_C$ receptors display little macroscopic desensitization. The very different waveforms indicate interesting variations. To evaluate the kinetic properties of the wild-type and mutant receptors, response waveforms were recorded at various GABA concentrations. Kinetic analysis of the wild-type receptor revealed a GABA concentration-dependent activation rate, with an apparent bimolecular rate constant (k_{act}) of 0.156 $\mu M^{-1}\ s^{-1}$ (Fig. 3*B* and Table 2). We consider that this parameter is reliable to ± 15%. As expected from most models, the deactivation phase for the $GABA_C$ receptor was well fitted by a single exponential and showed little or no concentration dependence (24, 25). This decay had a rate constant k_{deact} of 0.038 s^{-1}.

The single mutants E92Nha and E92D both show increased values for k_{act} and decreased values for k_{deact} (Fig. 3 (*C* and *D*) and Table 2). Both effects are larger for the more disruptive E92D mutant. The double mutant E92R/R258E has distinct

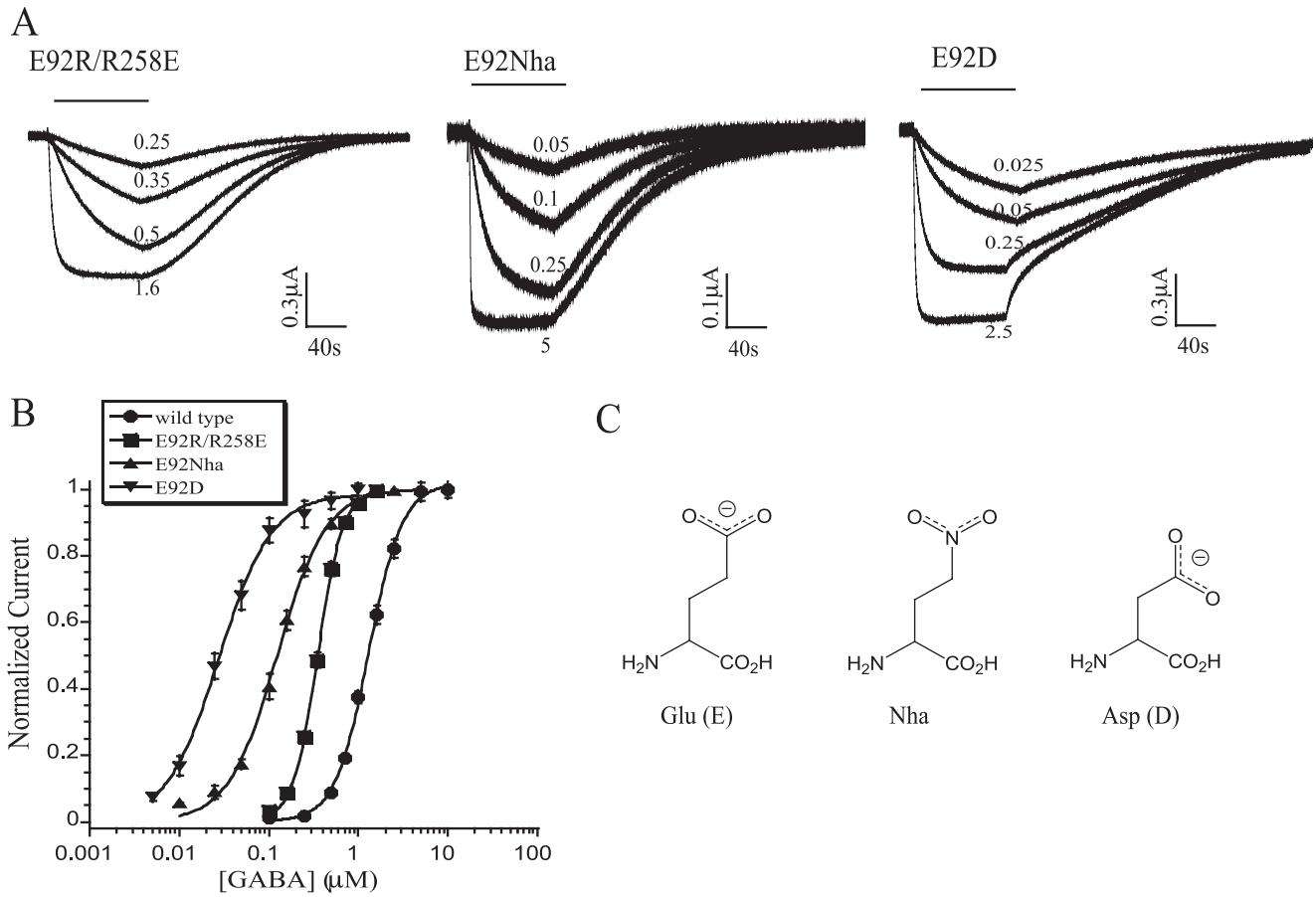

FIGURE 2. *A*, representative voltage-clamp current traces from oocytes expressing E92R/R258E (*left*), E92Nha (nitrohomoalanine, *middle*), and E92D (*right*). *Horizontal bars* represent application of GABA (micromolar). *B*, dose-response relations of GABA-mediated responses from oocytes expressing wild-type, E92R/R258E, E92Nha, and E92D receptors. EC_{50} and n_H values are given in Table 1. *C*, structures of Glu, Asp, and unnatural amino acid Nha.

kinetic properties (Fig. 3*E* and Table 2). The activation rate is roughly half that of wild type, and the deactivation rate is significantly decreased to one-fourth of the value for wild-type receptors.

The ρ1 GABA$_C$ receptor used in this study has a single-channel conductance of <2 pS (26, 27). The resulting small currents vitiate systematic kinetic studies using single-channel analysis.

Functional Properties of E92R/R258E and Wild-type Receptors—Because the E92R/R258E mutations we are evaluating occur at the gating interface and are quite remote from the agonist binding site (28), we expect changes in EC_{50} to reflect alteration of gating more than binding. To verify this, we compared several functional characteristics of the two receptors; the results are summarized in Table 3. The reversal potential of GABA currents mediated by the E92R/R258E mutant receptor was the same as for the wild-type receptor; both were close to -26 mV, indicating the currents are mainly carried by chloride, as expected. The GABA$_C$-competitive antagonist, TPMPA ((1,2,5,6-tetrahydropyridin-4-yl)methylphosphinic acid), reduced the GABA current with an IC_{50} of 1.7 μM for E92R/R258E, roughly 3-fold different from the wild-type receptor (5.5 μM). To examine the affinity of TPMPA for both receptors, Schild plots were generated (supplemental Fig. S2). K_d values obtained were 2.41 μM and 0.90 μM, for wild-type and mutant receptors, respectively, again a roughly 3-fold shift.

Zinc ion acts as an allosteric modulator of the GABA$_C$ receptor. Previous work has identified His-157 in the extracellular domain to be involved in Zn^{2+} block (29). Zinc ions blocked the E92R/R258E mutant receptor with an IC_{50} of 46 μM, whereas the IC_{50} for wild type was 52 μM, indicating that the mutant receptor does not disrupt down-modulation by zinc.

The behavior of the open channel blocker, picrotoxin, was also examined. Picrotoxin is considered to bind in the pore region of the receptor (30, 31). The E92R/R258E mutant channel is relatively insensitive to picrotoxin, with an 8-fold increase in IC_{50}.

Finally, we measured the relative efficacy (ϵ) of muscimol, a GABA$_C$ partial agonist, for wild-type receptors as well as the double mutant receptors (Table 3). The ϵ for the E92R/R258E receptor is substantially increased over that of the wild-type, from 0.61 to 1.09, converting muscimol from a partial agonist to a full agonist. In summary, for the E92R/R258E channel, the current is inhibited by TPMPA, down-modulated by Zn^{2+}, blocked by picrotoxin, and gated by muscimol, confirming the double mutant channel has the general pharmacological properties of the ρ1 receptors.

DISCUSSION

The present work reveals a significant ion pair interaction at the gating interface of the GABA$_C$ receptor. Although the sin-

gle mutant E92R is nonfunctional, and the single mutant R258E does not express on the cell surface, the double mutant E92R/R258E is fully functional, with an EC_{50} 4-fold less than wild type. In addition, the double mutant displays global functional and pharmacological characteristics that are typical for a $GABA_C$ ρ1 receptor. As noted earlier, the comparable pair, Glu^{45}–Arg^{209}, has been shown to interact in the muscle-type nAChR (15). Thus, unlike several other ion pairs of the gating interface that have been ascribed important roles in receptor function (12–14, 16), the pair considered here may well be important throughout the Cys-loop superfamily.

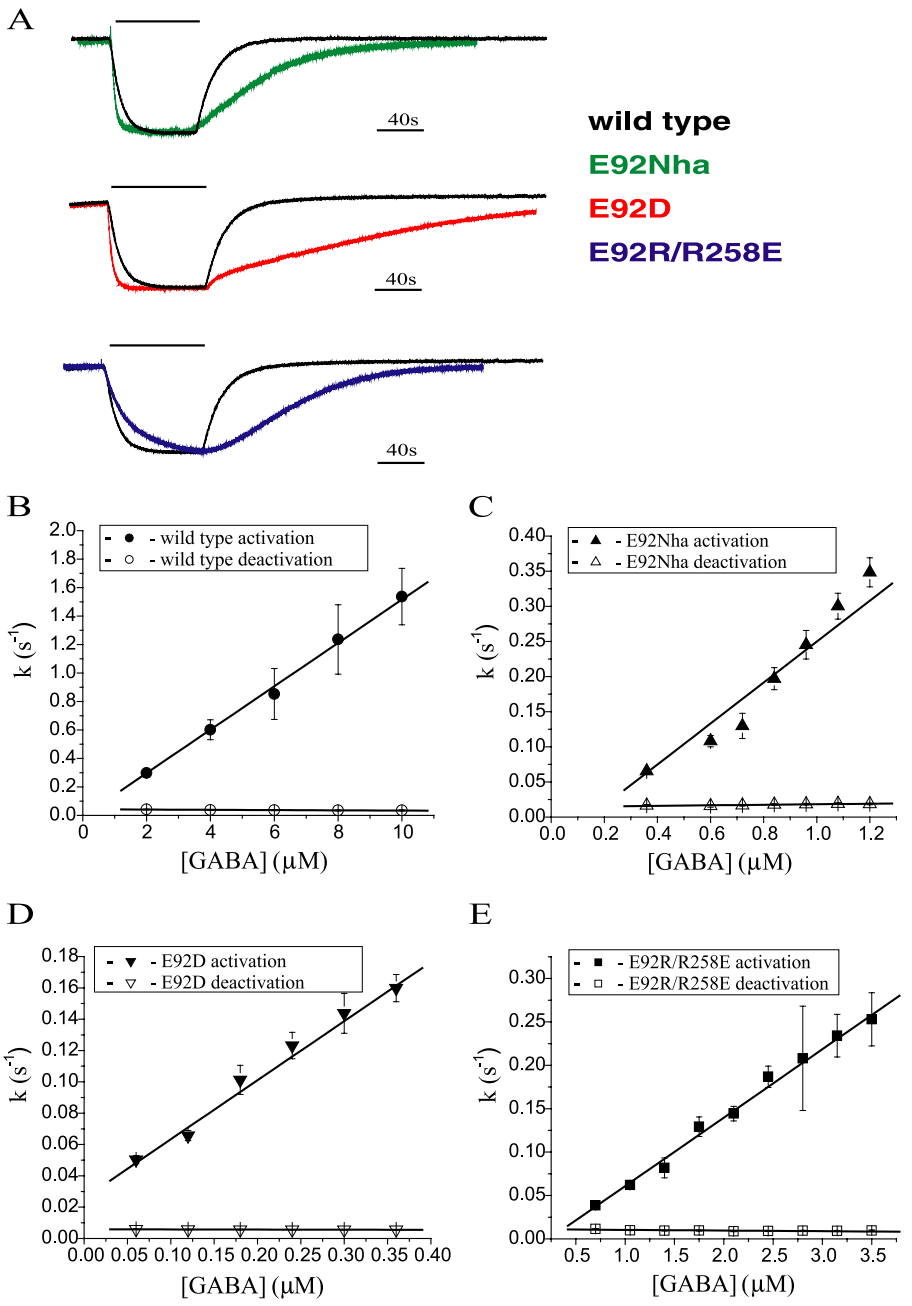

FIGURE 3. *A*, normalized current responses to 1 μM GABA from the oocyte expressing E92Nha (*green*), E92D (*red*), and E92R/R258E (*pink*), respectively, compared with wild-type receptor (*black*). *Bars* represent application of GABA. The *traces* show clearly the more rapid activation and slowly deactivation for both E92Nha and E92D receptors. The *traces* show the more slowly activation and deactivation for E92R/R258E receptors. *B*, kinetics properties of wild-type receptor. *C*, kinetics properties of E92Nha receptor. *D*, kinetics properties of E92D receptor. *E*, kinetics properties of E92R/R258E receptor.

That the Glu^{92}–Arg^{258} interaction really is an ion pair is supported by several observations. Note that the typical tool for establishing a pairwise interaction, a mutant cycle analysis (32), is not applicable here because the key single mutants do not produce functional receptors. Perhaps the most telling evidence for ion pairing results from the unnatural amino acid Nha. The side chain of Nha is isosteric and isoelectronic to that of glutamate; the only substantive difference is the lack of a negative charge. The Nha mutant shows an 11-fold decrease in EC_{50}, suggesting charge plays an important role. Note that, although unable to form an ion pair, the nitro group of Nha can hydrogen bond to the side chain of Arg^{258}. Although the hydrogen bond is expected to be 10- to 20-fold weaker than the analogous interaction with a carboxylate (20), this could account for the fact that the Nha receptor is still functional. Apparently, not only is the Glu^{92}–Arg^{258} interaction important, but it is also significantly geometrically constrained. The charge-conserving E92D mutation produces a larger EC_{50} shift than the charge-neutralizing Nha mutation. Apparently, the shorter Asp side chain *versus* Glu significantly compromises the Glu^{92}–Arg^{258} interaction. Because ion pairs are not usually considered to

TABLE 2
A comparison of kinetic parameters for the wild type, E92Nha, E92D, and E92R/R258E receptors

	k_{act}	$RT\ln(k_{act,WT}/k_{act,mut})$	k_{deact}	$RT\ln(k_{deact,WT}/k_{deact,mut})$
	$mM^{-1}\ s^{-1}$	*kcal mol*$^{-1}$	s^{-1}	*kcal mol*$^{-1}$
wild type	0.156 ± 0.006		0.038 ± 0.001	
E92Nha	0.28 ± 0.014	−0.35	0.017 ± 0.001	0.48
E92D	0.37 ± 0.024	−0.52	0.0057 ± 0.0001	1.12
E92R/R258E	0.079 ± 0.004	0.40	0.010 ± 0.001	0.79

TABLE 3

Functional comparison of wild-type and E92R/R258E receptors

GABA concentration for IC_{50} for wild-type and E92R/R258E is 4 μM and 1 μM (=EC_{95}), respectively. Schild plots are shown in supplemental Fig. S2.

	Wild type	E92R/R258E
Reversal potential (mV)	−27.1 ± 0.8	−25.9 ± 0.7
IC_{50} for TPMPA (μM)	5.5 ± 0.3	1.7 ± 0.1
n_H	1.8 ± 0.1	1.6 ± 0.1
K_d (μM)	2.41	0.90
IC_{50} for zinc (μM)	52 ± 2	46 ± 5
n_H	1.9 ± 0.1	1.5 ± 0.2
IC_{50} for picrotoxin (μM)	4.5 ± 0.2	37 ± 5
n_H	0.9 ± 0.03	0.7 ± 0.04
EC_{50} for muscimol (μM)	3.0 ± 0.1	0.56 ± 0.02
n_H	1.6 ± 0.1	2.5 ± 0.2
ϵ	0.61 ± 0.02	1.09 ± 0.03

be especially sensitive to distance, this significant effect suggests a substantial geometric constraint.

Several lines of evidence suggest that the Glu^{92}–Arg^{258} interaction plays a significant role in receptor gating. The double mutant E92R/R258E is functional, and it converts the partial agonist muscimol to a full agonist. Such observations are typically interpreted to mean that the mutation has affected the open probability of the receptor, such that a drug that cannot produce a large P_{open} for the wild-type receptor, a partial agonist, can do so for the double mutant. The 5-fold drop in EC_{50} of muscimol seen with the double mutant is completely consistent with this analysis. If we assume that binding of two ligands is required to efficiently gate the channel, the 60% efficacy of muscimol for the wild type indicates that the ratio of opening to closing rates, $\beta/\alpha = \Theta$, for the doubly liganded receptor is 1.5. Increasing this ratio to a value of 30, giving an efficacy of ~97%, would account for the 5-fold drop in EC_{50}, because this parameter varies as roughly the square root of Θ. We interpret the ~4-fold drop in EC_{50} for GABA activation to reflect a similar increase in Θ for the E92R/R258E mutant. Similar conclusions are reached if we assume binding of three ligands (see below).

The double mutant also affects the open channel blocker picrotoxin, raising IC_{50} by 8-fold. The picrotoxin binding site is in the channel region, far removed from the agonist binding site. In our interpretation of this finding, the double mutant has altered the structure in the gating region, not the agonist binding site. It is true that certain types of open-channel blockers are expected to show varying potency as Θ varies, even if the mutation changes the binding site; however, the most straightforward models predict that IC_{50} for a channel blocker would decrease as Θ increases (33). We believe that the lowered potency for picrotoxin does indicate that the Glu^{92}–Arg^{258} pair directly influences the binding of picrotoxin at a site within the channel region (30, 31).

Not surprisingly, modulation of the channel by Zn^{2+} is not affected by the E92R/R258E mutation, because the Zn^{2+} binding site is remote from both the agonist binding site and the channel gate. The competitive antagonist TPMPA does show an ~3-fold enhancement of binding in the double mutant. TPMPA is a larger molecule than GABA, and it may be that, while blocking the binding site, TPMPA can be closer to the Glu^{92}–Arg^{258} pair, such that it responds to mutations there either directly or through an allosteric effect.

As with other structural insights into receptors and receptor models, the image of the nAChR shown in Fig. 1 begs the question as to which state of the receptor we are viewing. Several lines of evidence suggest that, at least for the $GABA_C$ receptor, the ion pair probed here is present in the closed state and is broken on going to the open state. We assume the ion pair stabilizes the state in which it is present. Weakening the ion pair, either by charge neutralization (E92Nha) or by disrupting the geometry (E92D) destabilizes that state and lowers EC_{50}. The simplest way to interpret this is that weakening the Glu^{92}–Arg^{258} interaction destabilizes the closed state, which would thereby lower the barrier to the open state.

The homomeric ρ1 receptor displays activation and inactivation kinetics that are anomalously slow among Cys-loop receptor family members, although the actual kinetics appear to vary by up to 3-fold between oocyte and mammalian cell expression systems (34, 35). The previously available data do, however, agree in suggesting that the open state of the channel is much more likely to be associated with the presence of three or more bound GABA molecules than with fewer bound agonist molecules. Our interpretation that the highly sensitive E92D and E92Nha mutants have destabilized close states then suggests that the open state of the channel might require fewer bound agonist molecules. This hypothesis is consistent with our observation that the Hill coefficients of the dose-response relations decrease from the wild-type value of 2.2 to 1.4 and 1.6 for the highly sensitive mutants. Other explanations are possible, and we recognize that another mutant, R316D, is less sensitive than wild-type but it too has a lower Hill coefficient.

The macroscopic rate constants of Table 2 support this view of a destabilized closed state. These numbers are necessarily complex, with k_{act} reflecting a composite of binding and unbinding processes and channel opening (the latter is generally described by the rate constant β). That binding is involved is established by the increase in k_{act} with [GABA]. The requirement for multiple bound agonist molecules leads one to predict that k_{act} should increase more than linearly with [GABA] (33). However, this effect is expected to be most pronounced for [GABA] < EC_{50}, and for the usual reasons, our measurements are most precise at larger [GABA]. If we assume that mutations at Glu^{92}/Arg^{258} influence gating more than binding, as argued above, then *differences* in k_{act} can be ascribed to differences in β.

In contrast, k_{deact} is independent of [GABA]; so we associate this unimolecular rate constant with the rate constant for channel closing, α. With these assumptions about kinetics, the free energy diagrams of Fig. 4 can be constructed.

We assume that the ion pair is completely absent in the open state, and so the open state energy is unaffected by the mutations studied here. Then, the differences in k_{deact} set the relative positions of the transition states that separate open and closed states. The mutations destabilize the closed state. This destabilization must be more than the destabilization of the transition state by an amount that corresponds to the acceleration of the opening rate. That is, for E92Nha and E92D, the closed state must be destabilized by 0.48 + 0.35 = 0.83 kcal/mol and 1.12 + 0.52 = 1.64 kcal/mol, respectively. This simple model rational-

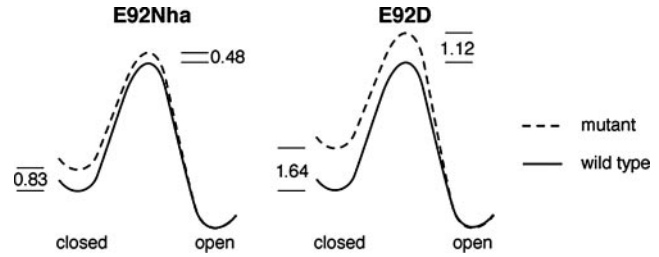

FIGURE 4. **Schematic energy diagram of the transition from the agonist bound closed state to open state of wild-type (*solid line*), E92Nha (*dashed line, left*), and E92D (*dashed line, right*).** Numbers are the free energy differences (kcal mol^{-1}) between wild-type and mutant receptor.

izes the acceleration of k_{act} and the deceleration of k_{deact} caused by mutations at Glu^{92}.

We can also estimate the extent to which the Glu^{92}–Arg^{258} interaction is present in the transition state for channel opening. For the E92Nha mutant, the value is 0.48/0.83 = 58%; for E92D it is 1.12/1.64 = 68%. The more severe E92D mutation produces an earlier transition state, as would be expected based on the greater destabilization of the starting (closed) state. Presumably, the wild-type receptor would have a later transition state than either mutant, perhaps with ~50% of the ion pair interaction present. This value is consistent with Auerbach's free energy analyses of residues in this region, which establish Φ values that are intermediate between those of the agonist binding site region and those of the transmembrane region (36, 37).

In summary, we have established an important ion pair interaction between Glu^{92} and Arg^{258} in the gating interface of the $GABA_C$ receptor, the second example of this interaction being important in a Cys-loop receptor. Several lines of reasoning and earlier work suggest that the ion pair probed here plays an important role in channel gating. We propose that the Glu^{92}–Arg^{258} ion pair stabilizes the closed state of the receptor and is completely broken upon going to the open state. Free energy analysis suggests the ion pair is ~50% broken at the gating transition state, consistent with other models of receptor activation.

Acknowledgment—We thank Michael Torrice for the preparation of Nha.

REFERENCES

1. Bormann, J. (2000) *Trends Pharmacol. Sci.* **21,** 16–19
2. Chebib, M., and Johnston, G. A. (2000) *J. Med. Chem.* **43,** 1427–1447
3. Cutting, G. R., Lu, L., O'Hara, B. F., Kasch, L. M., Montrose-Rafizadeh, C., Donovan, D. M., Shimada, S., Antonarakis, S. E., Guggino, W. B., Uhl, G. R., and Kazazian, Jr., H. H. (1991) *Proc. Natl. Acad. Sci. U. S. A.* **88,** 2673–2677
4. Boue-Grabot, E., Roudbaraki, M., Bascles, L., Tramu, G., Bloch, B., and Garret, M. (1998) *J. Neurochem.* **70,** 899–907
5. Wegelius, K., Pasternack, M., Hiltunen, J. O., Rivera, C., Kaila, K., Saarma, M., and Reeben, M. (1998) *Eur. J. Neurosci.* **10,** 350–357
6. Enz, R., Brandstatter, J. H., Hartveit, E., Wassle, H., and Bormann, J. (1995) *Eur. J. Neurosci.* **7,** 1495–1501
7. Lester, H. A., Dibas, M. I., Dahan, D. S., Leite, J. F., and Dougherty, D. A. (2004) *Trends Neurosci.* **27,** 329–336
8. Brejc, K., van Dijk, W. J., Klaassen, R. V., Schuurmans, M., van der Oost, J., Smit, A. B., and Sixma, T. K. (2001) *Nature* **411,** 269–276
9. Unwin, N. (2005) *J. Mol. Biol.* **346,** 967–989
10. Miyazawa, A., Fujiyoshi, Y., and Unwin, N. (2003) *Nature* **423,** 949–955
11. Unwin, N., Miyazawa, A., Li, J., and Fujiyoshi, Y. (2002) *J. Mol. Biol.* **319,** 1165–1176
12. Absalom, N. L., Lewis, T. M., Kaplan, W., Pierce, K. D., and Schofield, P. R. (2003) *J. Biol. Chem.* **278,** 50151–50157
13. Kash, T. L., Dizon, M. J. F., Trudell, J. R., and Harrison, N. L. (2004) *J. Biol. Chem.* **279,** 4887–4893
14. Kash, T. L., Jenkins, A., Kelley, J. C., Trudell, J. R., and Harrison, N. L. (2003) *Nature* **421,** 272–275
15. Lee, W. Y., and Sine, S. M. (2005) *Nature* **438,** 243–247
16. Xiu, X. N., Hanek, A. P., Wang, J. T., Lester, H. A., and Dougherty, D. A. (2005) *J. Biol. Chem.* **280,** 41655–41666
17. Sala, F., Mulet, J., Sala, S., Gerber, S., and Criado, M. (2005) *J. Biol. Chem.* **280,** 6642–6647
18. Liman, E. R., Tytgat, J., and Hess, P. (1992) *Neuron* **9,** 861–871
19. McMenimen, K. A., Dougherty, D. A., Lester, H. A., and Petersson, E. J. (2006) *ACS Chem. Biol.* **1,** 227–234
20. Cashin, A. L., Torrice, M. M., McMenimen, K. A., Lester, H. A., and Dougherty, D. A. (2007) *Biochemistry* **46,** 630–639
21. Cashin, A. L., Petersson, E. J., Lester, H. A., and Dougherty, D. A. (2005) *J. Am. Chem. Soc.* **127,** 350–356
22. Vicente-Agullo, F., Rovira, J. C., Sala, S., Sala, F., Rodriguez-Ferrer, C., Campos-Caro, A., Criado, M., and Ballesta, J. J. (2001) *Biochemistry* **40,** 8300–8306
23. Castaldo, P., Stefanoni, P., Miceli, F., Coppola, G., Del Giudice, E. M., Bellini, G., Pascotto, A., Trudell, J. R., Harrison, N. L., Annunziato, L., and Taglialatela, M. (2004) *J. Biol. Chem.* **279,** 25598–25604
24. Qian, H., Dowling, J. E., and Ripps, H. (1998) *J. Neurobiol.* **37,** 305–320
25. Qian, H., Dowling, J. E., and Ripps, H. (1999) *J. Neurobiol.* **40,** 67–76
26. Zhu, Y., Ripps, H., and Qian, H. (2007) *Neurosci. Lett.* **418,** 205–209
27. Wotring, V. E., Chang, Y., and Weiss, D. S. (1999) *J. Physiol.* **521,** 327–336
28. Lummis, S. C. R., Beene, D. L., Harrison, N. J., Lester, H. A., and Dougherty, D. A. (2005) *Chem. Biol.* **12,** 993–997
29. Wang, T. L., Hackam, A., Guggino, W. B., and Cutting, G. R. (1995) *J. Neurosci.* **15,** 7684–7691
30. Wang, T. L., Hackam, A. S., Guggino, W. B., and Cutting, G. R. (1995) *Proc. Natl. Acad. Sci. U. S. A.* **92,** 11751–11755
31. Zhang, D., Pan, Z. H., Zhang, X., Brideau, A. D., and Lipton, S. A. (1995) *Proc. Natl. Acad. Sci. U. S. A.* **92,** 11756–11760
32. Hidalgo, P., and MacKinnon, R. (1995) *Science* **268,** 307–310
33. Adams, D. J., Nonner, W., Dwyer, T. M., and Hille, B. (1981) *J. Gen. Physiol.* **78,** 593–615
34. Yang, J., Cheng, Q., Takahashi, A., and Goubaeva, F. (2006) *Biophys. J.* **91,** 2155–2162
35. Chang, Y., and Weiss, D. S. (1999) *Nat. Neurosci.* **2,** 219–225
36. Auerbach, A. (2003) *Sci. STKE* **2003,** re11
37. Chakrapani, S., Bailey, T. D., and Auerbach, A. (2004) *J. Gen. Physiol.* **123,** 341–356